Plasticity and Stereotypic Rewiring of the Transcriptome Upon Bacterial Evolution of Antibiotic Resistance

Gábor Grézal,[1,2] Réka Spohn,[2] Orsolya Méhi,[2,3] Anett Dunai,[2] Viktória Lázár,[2,4] Balázs Bálint,[2,5] István Nagy [5,6] Csaba Pál,[2,7] and Balázs Papp [*,1,2,8]

[1]HCEMM-BRC Metabolic Systems Biology Lab, Szeged, Hungary

[2]Synthetic and Systems Biology Unit, Institute of Biochemistry, Biological Research Centre, Eötvös Loránd Research Network, Szeged, Hungary

[3]HCEMM-BRC Translational Microbiology Research Lab, Szeged, Hungary

[4]HCEMM-BRC Pharmacodynamic Drug Interaction Research Group, Szeged, Hungary

[5]SeqOmics Biotechnology Ltd., Mórahalom, Hungary

[6]Sequencing Platform, Institute of Biochemistry, Biological Research Centre, Eötvös Loránd Research Network, Szeged, Hungary

[7]National Laboratory of Biotechnology, Biological Research Centre, Eötvös Loránd Research Network, Szeged, Hungary

[8]National Laboratory for Health Security, Biological Research Centre, Eötvös Loránd Research Network, Szeged, Hungary

***Corresponding author:** E-mail: pappb@brc.hu.

Associate editor: Miriam Barlow

Abstract

Bacterial evolution of antibiotic resistance frequently has deleterious side effects on microbial growth, virulence, and susceptibility to other antimicrobial agents. However, it is unclear how these trade-offs could be utilized for manipulating antibiotic resistance in the clinic, not least because the underlying molecular mechanisms are poorly understood. Using laboratory evolution, we demonstrate that clinically relevant resistance mutations in *Escherichia coli* constitutively rewire a large fraction of the transcriptome in a repeatable and stereotypic manner. Strikingly, lineages adapted to functionally distinct antibiotics and having no resistance mutations in common show a wide range of parallel gene expression changes that alter oxidative stress response, iron homeostasis, and the composition of the bacterial outer membrane and cell surface. These common physiological alterations are associated with changes in cell morphology and enhanced sensitivity to antimicrobial peptides. Finally, the constitutive transcriptomic changes induced by resistance mutations are largely distinct from those induced by antibiotic stresses in the wild type. This indicates a limited role for genetic assimilation of the induced antibiotic stress response during resistance evolution. Our work suggests that diverse resistance mutations converge on similar global transcriptomic states that shape genetic susceptibility to antimicrobial compounds.

Article

Introduction

Excessive use of antibiotics promotes the rapid evolution of resistant bacteria that eventually limit the clinical use of existing antibiotics. However, antibiotic resistance mutations frequently come at various costs that shape their selective advantage. First, resistance often induces a fitness cost in the absence of antibiotic stress (Andersson and Hughes 2010; Dunai et al. 2019). Second, resistance to specific antibiotics frequently increases sensitivity to various other antibiotics and antimicrobial peptides (Lázár et al. 2013; Imamovic et al. 2018) a phenomenon termed collateral sensitivity (Pál et al. 2015). Third, resistance mutations in pathogens can diminish tolerance to stresses from the host environment and thereby reduce virulence (Vincent et al. 2013). Collectively, such fitness trade-offs offer evolutionary strategies to diminish or even reverse the selective advantage of resistant microbes (Pál et al. 2015; Baym et al. 2016). A better understanding of antibiotic resistance trade-offs is therefore crucial for the design of evolution-proof antimicrobial therapies.

Mounting evidence indicates that gene expression alterations play an important role in mediating the trade-offs of resistance mutations (Webber et al. 2013; Suzuki et al. 2014). For example, in a set of laboratory-evolved bacteria, resistance to various antibiotics was predictable based on the gene expression levels of a small set of genes (Suzuki et al. 2014). Antibiotic resistance mutations might also induce global transcriptomic changes and, as a by-product, influence the expression level of various other genes underlying antibiotic susceptibility. For example, a clinically relevant mutation in the topoisomerase gene *gyrA* confers resistance to fluoroquinolones and simultaneously changes the expression of numerous genes via altered DNA supercoiling (Webber et al. 2013). However, despite the potential importance of genomic expression patterns in shaping antibiotic resistance profiles, we have only a limited understanding of the global transcriptomic

rewiring induced by resistance mutations. First of all, it remains unknown whether expression changes affecting hundreds of genes across the genome is the exception or the rule. Second, it is unknown whether the transcriptional changes induced by antibiotic stress can later become genetically fixed in the population by natural selection. An analogous process, termed genetic assimilation, has been observed for a range of inducible phenotypic characters (Waddington 1961; Schlichting and Wund 2014; Vigne et al. 2021). Under the assumption that genetic assimilation acts on transcriptome evolution, one might expect that the transcriptional states caused by resistance mutations *in the absence of a given antibiotic stress* (i.e., constitutive or genetically encoded) should be similar to those induced by the same antibiotic in the susceptible wild-type genetic background. Third, while bacteria adapted to different antibiotics often show overlap in their sets of mutated genes (Toprak et al. 2012; Lázár et al. 2014), the extent of parallel evolution at the transcriptomic level is poorly studied. Finally, the phenotypic consequences of global transcriptomic changes are largely uncharted.

In this work, we explore the general patterns and phenotypic associations of transcriptomic changes induced by antibiotic adaptation by focusing on a set of laboratory-evolved *Escherichia coli* lines generated in our previous study (Lázár et al. 2014). This panel of lines covers adaptations to a range of clinically relevant antibiotics and is well-characterized with available whole-genome sequences and resistance phenotypes (Lázár et al. 2013, 2014). Our analyses led to five major conclusions. First, we find that resistance conferring mutations generally induce global transcriptomic changes that span hundreds of genes. Second, genomic expression levels tend to change in a parallel manner across lines adapted to antibiotics with different modes of action, yielding a small number of recurrent gene expression signatures. Third, parallel transcriptomic changes are largely decoupled from parallel changes in mutated genes and resistance pathways. Thus, there are multiple alternative routes to evolve a "stereotypic" expression state during antibiotic adaptation, with each demanding a small number of mutations in functionally diverse genes. Fourth, such recurring gene expression changes typically affect oxidative stress regulation, iron homeostasis and pathways underlying outer membrane and cell surface composition. As a consequence, genotypes with extensive genomic expression changes show elongated cell shape and increased sensitivity to various antimicrobial peptides. Finally, the constitutive transcriptomic changes induced by resistance mutations in the absence of antibiotic stress do not resemble those induced by antibiotic stresses in the susceptible wild-type background, indicating a limited role for genetic assimilation of the antibiotic stress response during resistance evolution.

Results

Adaptation to Antibiotics Generally Induce Global Transcriptome Rewiring

To explore the extent of transcriptomic changes caused by antibiotic resistance mutations, we analyzed transcriptomic data of a set of well-characterized laboratory-evolved resistant *E. coli* K-12 BW25113 lines. Specifically, in our previous study, ten parallel *E. coli* populations derived from a common ancestor were exposed to gradually increasing concentrations of one of 12 clinically relevant antibiotics with diverse modes of actions (table 1; Lázár et al. 2013, 2014). After ~240–384 generations, all adapted lines showed a substantial increase in resistance, with up to 328-fold increases in their minimum inhibitory concentrations (MICs) relative to the wild type (Lázár et al. 2014). Whole-genome resequencing showed that most mutations accumulated in the adapted lines were driven by selection and many had also been detected in antibiotic-resistant clinical isolates (Lázár et al. 2014). Here, we focused on a set of 24 antibiotic-adapted lines, two parallel lines per each of the 12 antibiotics, for which transcriptomic (RNA-Seq) and whole-genome sequence data were generated in our previous studies (Lázár et al. 2013, 2014, 2018). RNA samples were collected in antibiotic-free medium to ensure comparability between lines that display vastly different resistance levels (Lázár et al. 2018). Thus, in this study, evolution of transcriptomic states corresponds to constitutive gene expression changes that are manifested in the absence of antibiotic stress. Note that none of the antibiotic-adapted lines analyzed here are hypermutators (supplementary data S1, Supplementary Material online).

We report that 5–33% (on average, ~20%) of the 4,293 studied genes are significantly up- or downregulated in antibiotic-adapted lines (i.e., show at least a two-fold change [FC] with an FDR-adjusted $P < 0.05$, see fig. 1A). Both up- and downregulations show similar extents of transcriptional changes across lines (Pearson's $r = 0.91$,

Table 1. List of Antibiotic-adapted *Escherichia coli* Lines Evolved in the Laboratory.

Genotype	Antibiotics used during adaptation	Mode of action
AMP7	Ampicillin	Cell-wall synthesis
AMP9		
FOX1	Cefoxitin	
FOX8		
CPR4	Ciprofloxacin	Gyrase inhibitor
CPR9		
NAL6	Nalidixic acid	
NAL8		
NIT6	Nitrofurantoin	Multiple mechanisms
NIT7		
CHL2	Chloramphenicol	Protein synthesis
CHL9		
ERY2	Erythromycin	
ERY6		
DOX2	Doxycycline	Protein synthesis
DOX5		
TET1	Tetracycline	
TET7		
TRM6	Trimethoprin	Folic acid biosynthesis
TRM7		
TOB8	Tobramycin	Aminoglycoside
TOB9		
KAN1	Kanamycin	
KAN4		

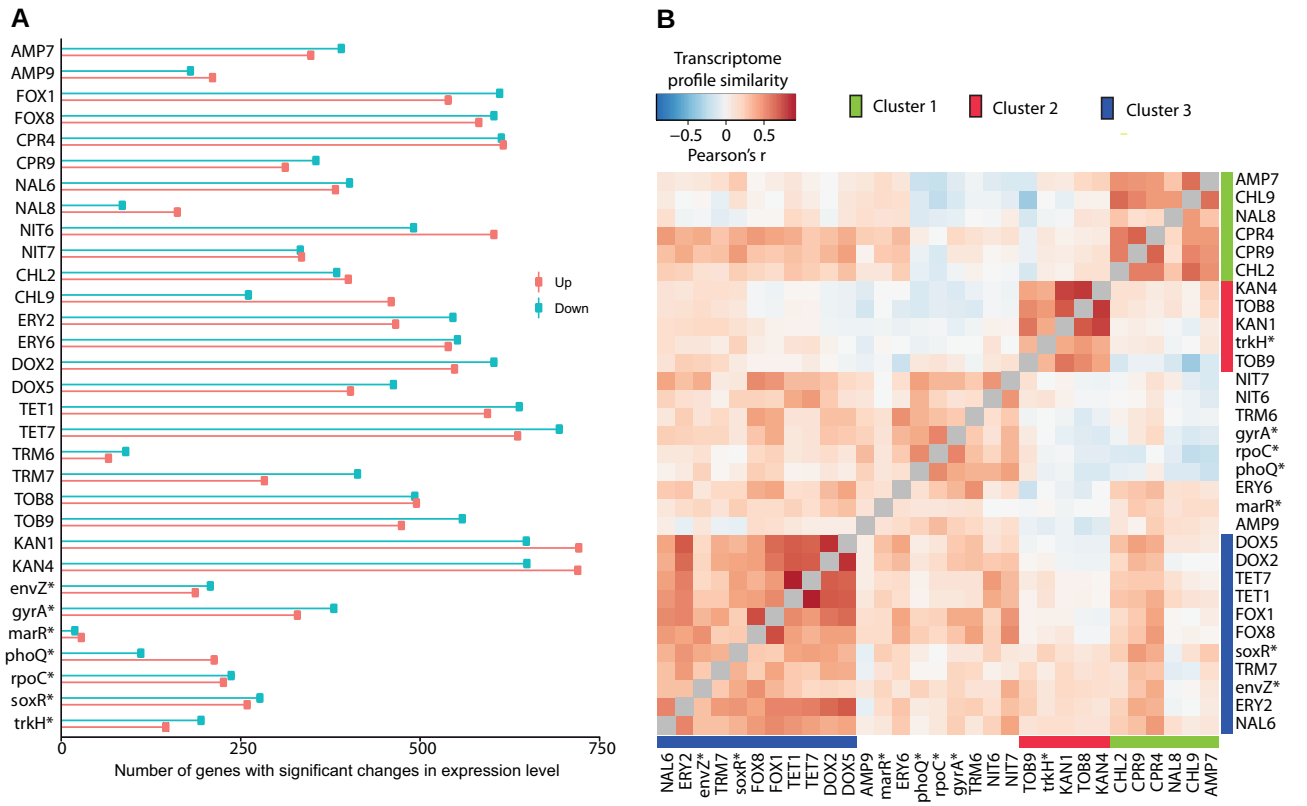

Fig. 1. Extensive and parallel gene expression changes in antibiotic-adapted and single-mutant genotypes. Gene expression analysis of the 24 antibiotic-adapted and 7 single-mutant genotypes. (*A*) Plot shows the number of significantly up- (red) or downregulated (blue) genes (FC > 2 or <0.5 and FDR-corrected *P*-value < 0.05) for each genotype. (*B*) Heatmap shows transcriptome similarities between all investigated genotypes. Clustering was performed using the Ward method and using 1 − Pearson's r correlation coefficient as a distance measure (Murtagh and Legendre 2014, Materials and Methods). Colored stripes along the heatmap's axes indicate clusters of elevated transcriptomic similarity.

$P < 0.0001$). Moreover, the proportions of significantly altered genes are comparable with those reported in response to various environmental stresses (7–27% of genes; Jozefczuk et al. 2010). Importantly, the extent of transcriptional rewiring observed in the antibiotic-adapted lines is comparable with that of previously identified mutations with global transcriptomic impact. For example, a specific resistance mutation in a gyrase gene globally changes the supercoiling state of the DNA and alters expression in 10% of genes in *Salmonella enterica* (Webber et al. 2013).

The above results suggest that resistance mutations frequently cause global transcriptomic changes. Two lines of evidence indicate that certain resistance mutations have especially large impact on the extent of global transcriptomic changes. First, we found that the extent of transcriptomic rewiring does not correlate with the number of mutations accumulated during evolution (supplementary fig. S1A, Supplementary Material online). Second, we experimentally tested whether a single resistance mutation is sufficient to induce global transcriptomic rewiring. To this end, we focused on a set of seven engineered lines that differ from the wild type by single mutations only and were constructed in our previous study (Lázár et al. 2014; table 2). These mutations reside in genes that have been repeatedly mutated across the antibiotic-adapted lines, cover a range of molecular functions and confer resistance to multiple antibiotics (Lázár et al. 2013, 2014). Importantly, several of these genes have been previously found to be mutated in antibiotic-resistant clinical isolates, highlighting their clinical relevance (e.g., *acrAB* and *tolC* [Piddock 2006], *gyrA* [Vila et al. 1994], *ompF* and *marR* [Randall and Woodward 2002], *soxRS* [Webber and Piddock 2001; Koutsolioutsou et al. 2005], and *envZ* [Adler et al. 2016]). Next, we measured the transcriptomes of these seven lines in antibiotic-free medium using the same pipeline as for the 24 antibiotic-adapted lines (see Materials and Methods, supplementary data S2, Supplementary Material online). We found that the single mutants often show widespread transcriptomic changes (on average, 9.5% of the genes are altered, see fig. 1A). Notably, while a specific mutation in *gyrA* causes the largest transcriptomic effect (17% of genes), resistance mutations in other genes also induce widespread regulatory rewiring, including mutations in *envZ*, which is a member of the two-component regulatory system involved in osmotic stress (Mizuno and Mizushima 1990; Seo et al. 2017) and transcriptional regulator SoxR (Wu and Weiss 1991; Koutsolioutsou et al. 2005).

Slow cellular growth is frequently associated with global gene expression changes (Matsumoto et al. 2013; Schmidt et al. 2016), and resistance mutations often decrease growth rate by incurring a fitness cost (Andersson and

Table 2. List of Genotypes Engineered to Carry Single Resistance Mutations.

Genotype	Mutation	Description of the genes
envZ*	Val241Gly	Sensory histidine kinase
gyrA*	Asp87Gly	DNA gyrase subunit A
marR*	Val84Glu	DNA-binding transcriptional repressor
phoQ*	Gly384Cys	Bifunctional sensory histidine kinase
rpoC*	Ala784Val	RNA polymerase subunit β'
soxR*	Leu139*	DNA-binding transcriptional dual regulator
trkH*	Thr350Lys	K+ transporter

Levin 1999; Dunai et al. 2019). However, two lines of observations indicate that the observed widespread transcriptomic alterations are unlikely to be induced by the fitness cost of resistance mutations. First, previous growth rate measurements of the same antibiotic-adapted lines revealed that substantial fitness costs are infrequent and are mostly associated with aminoglycoside adaptation (supplementary data S3, Supplementary Material online; Dunai et al. 2019). Second, we found no significant correlation between relative fitness and the total number of transcriptionally altered genes (Spearman's rho = −0.15, $P = 0.48$, see supplementary fig. S1*B*, Supplementary Material online). Taken together, adaptation to antibiotic stress results in global transcriptomic changes in the absence of antibiotics and this effect is not simply the by-product of slow growth of resistant bacteria.

Pervasive Parallel Transcriptomic Evolution Across Antibiotic Stresses

Previous works established that evolution toward increased antibiotic resistance is often achieved through genes that are repeatedly mutated in independently evolving lineages, resulting in parallel evolution at the molecular level (Koutsolioutsou et al. 2005; Toprak et al. 2012; Lázár et al. 2013; Webber et al. 2013; Oz et al. 2014). Here we sought to assess the extent of parallel evolution at the level of the transcriptomic changes, both within and between antibiotics. To this end, we measured transcriptome similarity between genotypes by calculating the Pearson correlation coefficient between their pairwise gene expression profiles. Clustering of the 24 antibiotic-adapted lines based on their transcriptome similarities revealed three major patterns. First, genotypes adapted to the same antibiotic have a tendency to cluster together on the heatmap (fig. 1*B*). Second, lines adapted to aminoglycosides show transcriptional profiles that are highly dissimilar from the rest of antibiotic -adapted lines (average Pearson's $r = 0.03$), but are highly similar among each other (see Cluster 2 on fig. 1*B*). Aminoglycosides have distinct resistance mechanisms and a uni que uptake pathway (Taber et al. 1987). Indeed, the sets of genes mutated in aminoglycoside-adapted lines show virtually no overlap with those mutated in other lines (Lázár et al. 2014). Third, lines adapted to various classes of antibiotics converge on a limited number of transcriptomic clusters (fig. 1*B*), indicating widespread parallel evoluti on of gene expression upon diverse antibiotic stresses.

To further investigate the extent of parallel evolution, we compared the transcriptome profile similarities of lines adapted to the same antibiotic (within drugs), lines adapted to different antibiotics that have the same mode of action (within classes), and lines adapted to different drugs with different modes of action (between classes; fig. 2*A*). This analysis confirmed that, on average, parallel gene expression changes are strongest between genotypes that were exposed to the same antibiotic (fig. 2*B*). This result remains when excluding aminoglycoside-adapted lines (fig. 2*C*), which show similar transcriptome profiles to each other but are highly distinct from the rest of adapted lines. The extent of parallel evolution between lines that were exposed to the same antibiotic differs across antibiotic classes: lines adapted to 30S ribosome inhibitors tetracycline and doxycycline show especially strong signals of parallel transcriptomic changes (supplementary fig. S2, Supplementary Material online).

Strikingly, we find that even lines adapted to different classes of antibiotics often show a positive Pearson correlation in their transcriptome profiles (average Pearson's $r = 0.22$). This pattern is especially prominent when excluding aminoglycoside-adapted lines (fig. 2*C*): on average, two lines adapted to distinct non-aminoglycoside antibiotic classes show a profile similarity of $r = 0.29$. These results apply to both up- and downregulations of gene expression (supplementary fig. S2, Supplementary Material online). For example, nalidixic acid–adapted lines show a ∼fourfold enrichment in upregulated genes with lines adapted to other antibiotic classes (supplementary fig. S2, Supplementary Material online). Although we observed a general tendency of lines adapted to distinct antibiotic classes to have similar transcriptomes, such similarities are not evenly distributed (fig. 1*B*). Specifically, the majority of non-aminoglycoside-adapted lines form two clusters of elevated transcriptomic similarity, encompassing six and nine adapted lines, respectively (see fig. 1*B*). Importantly, both clusters contain lines adapted to multiple distinct antibiotic classes. Overall, these findings suggest widespread parallel evolution of gene expression as a response to antibiotic adaptation, even upon exposure to antibiotics with different modes of action.

Evolutionary Changes Do Not Resemble Plastic Gene Expression Changes Initiated by Antibiotic Treatments

Evolutionary adaptation to a new stressful environment may begin with environmentally initiated phenotypic changes without the involvement of mutations (i.e., phenotypic plasticity), followed by beneficial genetic changes. If the plastic phenotypic response enhances fitness in the new stressful environment, it might be selected to become constitutively expressed without the stress cue, a process termed genetic assimilation (Waddington 1953; Schlichting and Wund 2014; Ehrenreich and Pfennig 2016). More specifically, plastic transcriptomic changes initiated by sublethal doses of antibiotics may enhance cell survival and may be assimilated by genetic changes driven

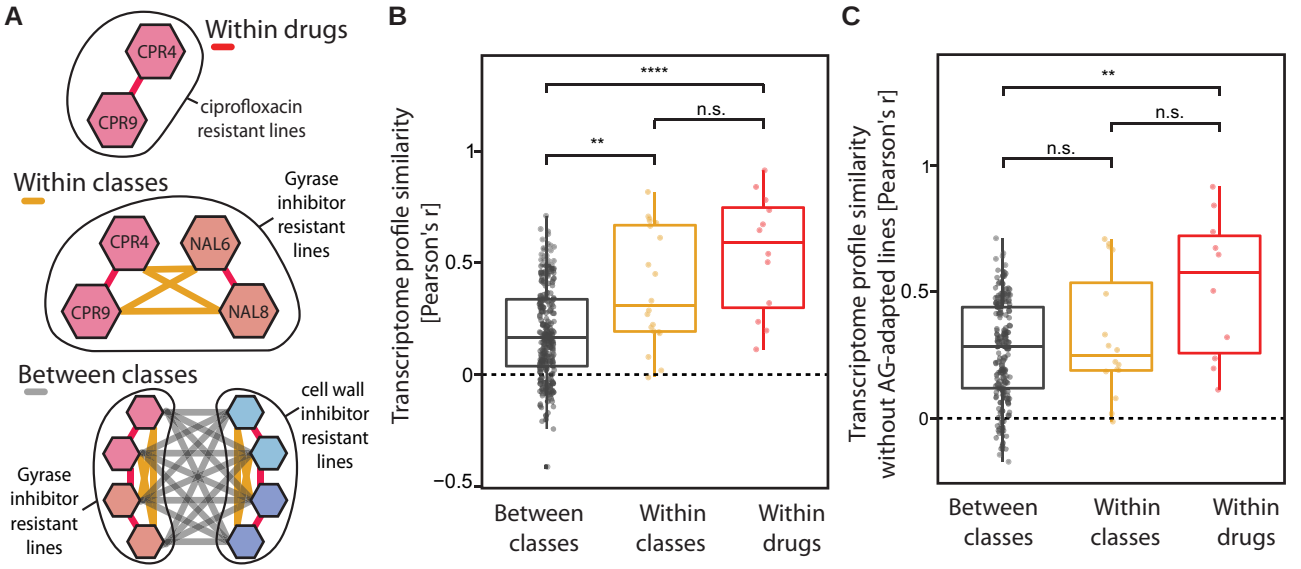

Fig. 2. Parallel evolution of gene expression changes. (*A*) Pairs of antibiotic-adapted lines were classified as follows: within-drugs (red line) when both lines were adapted to the same antibiotic, within-classes (orange line) when lines were adapted to different antibiotics with the same mode of action, or between classes (gray line) when lines were adapted to antibiotics with different modes of action. (*B*) Between-class line pairs show lower transcriptome profile similarity (Pearson's *r*) than those in within-drugs or within-classes (****$P < 0.0001$ and ** $P < 0.01$, Welch's test). Transcriptome profile similarity was defined by pairwise correlation of the gene expression profiles. (*C*) Within-drug line pairs show significantly higher transcriptome profile similarity than between-classes line pairs even when excluding aminoglycoside-adapted lines (**$P < 0.01$, Welch's test). However, between-class similarity no longer differs from within-class similarity due to the increased similarity of between-class pairs upon exclusion of aminoglycoside-adapted lines.

by natural selection to tolerate antibiotic stress, resulting in the constitutive expression of the initial gene expression changes. If different antibiotics induce similar plastic transcriptomic responses (Kohanski et al. 2007), then genetic assimilation might explain the pervasive parallel evolution of constitutive transcriptomic changes across antibiotics stresses. To test this idea, we analyzed a published data set of transcriptomic responses of wild-type *E. coli* to various sublethal antibiotic treatments, including five antibiotics studied here (Zoffmann et al. 2019; fig. 3). Note that the strain background (BW25113) employed in the transcriptomic study was the same as the ancestor strain in our evolutionary experiments. We found that antibiotic treatments generally induce widespread transcriptional changes in the wild type (on average, ~845 differentially expressed genes, supplementary table S1, Supplementary Material online), and different antibiotics tend to elicit similar expression responses (average Pearson's $r = 0.35$), as expected based on earlier observations (Kohanski et al. 2007; fig. 3). However, the transcriptomic changes of antibiotic-adapted lines in the absence of antibiotic stress show very low overall similarities with the plastic transcriptome responses induced by the corresponding antibiotics (average Pearson's $r = 0.07$), with a nitrofurantoin-adapted line being the sole exception (Pearson's $r = 0.4$). To test whether the low similarity between the evolved constitutive and the plastic transcriptional states holds upon high antibiotic dose, we next measured the transcriptomic response of the ancestral strain to lethal ciprofloxacin treatment (i.e., at a six-fold MIC concentration) using the same transcriptomic protocol as for the evolved lines (see Materials and Methods and fig. 3). Specifically, we investigated gene expression changes after 120 min of lethal ciprofloxacin stress in the ancestral wild-type background (see Materials and Methods). Again, we found very low overall similarities between the plastic transcriptional responses and the constitutive transcriptomic changes evolved in the two ciprofloxacin-adapted lines (Pearson's $r = 0.06$ and −0.08 for CPR4 and CPR9, respectively). Together, these results indicate that genetic assimilation of the plastic transcriptomic changes initiated by antibiotic stresses is unlikely to explain the frequent convergence of constitutive gene expression states following resistance evolution.

Genomic and Transcriptomic Parallel Evolution are Largely Decoupled

We next explored the links between parallel evolution at the genomic and the transcriptomic levels. One might expect that parallel gene expression changes are caused by parallel mutated genes in the different antibiotic-adapted lines. To assess the role of parallel mutated genes in transcriptome similarity, we asked whether the number of shared mutated genes explains transcriptome similarity between the antibiotic-adapted lines. Because aminoglycoside-adapted lines show dissimilar transcriptome profiles (fig. 1*B*) and also carry highly distinct mutations, we exclude them from all subsequent analyses. Remarkably, the number of shared mutated genes does not correlate with transcriptome similarity (Spearman's rho = 0.11, $P = 0.14$, fig. 4*A*). Importantly, many pairs of antibiotic-adapted lines do not share any mutated

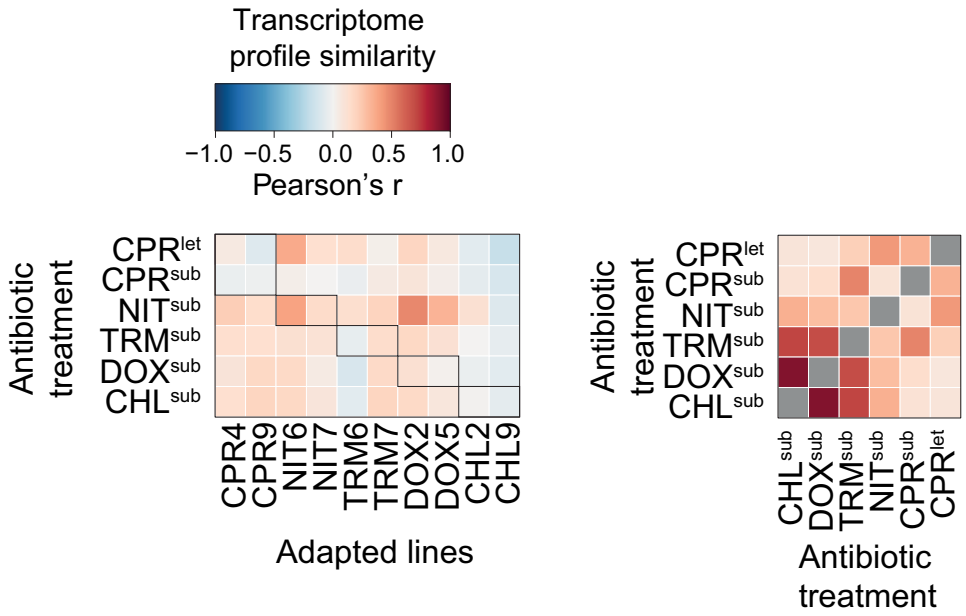

Fig. 3. Plastic and evolutionary changes in the transcriptome are largely distinct. Gene expression changes in the ancestor BW25113 strain background induced by lethal (let) ciprofloxacin treatment (supplementary data S2, Supplementary Material online) and by sublethal (sub) treatment with five antibiotics from a previous study (supplementary data S2, Supplementary Material online; Zoffmann et al. 2019). Heatmap on the left shows transcriptome similarities between antibiotic treatments and corresponding antibiotic-adapted lines, while the heatmap on the right shows transcriptome similarities between antibiotic treatments. Gray cells along the diagonal of the right heatmap represent self-comparisons that have been omitted. Tiles outlined with black rectangles highlight relevant comparisons, that is similarity between an antibiotic treatment and evolutionary adaptation to the same antibiotic.

genes, yet they show a substantial degree of transcriptome similarity (i.e., 30% of such pairs have a Pearson's $r > 0.4$).

To further test whether completely different sets of mutations can result in similar transcriptomic states, we next compared the transcriptomes of engineered strains carrying specific single resistance mutations with antibiotic-adapted lines that do not carry any mutations in the corresponding genes (supplementary data S3, Supplementary Material online). We found several cases, spanning multiple antibiotic classes and resistance mechanisms, where an engineered mutant strain shows marked transcriptome similarity to an antibiotic-adapted line with no shared mutated gene. For example, the transcriptome profiles of strain pairs FOX8-envZ*, CPR9-soxR*, NIT7-phoQ*, TET7-soxR*, DOX2-soxR*, TET1-soxR*, and FOX1-gyrA* all display a Pearson correlation >0.4. Manual inspection of the deposited sequence data of these adapted lines confirmed that the corresponding genes remained intact during laboratory evolution (supplementary data S1 and S3, Supplementary Material online). We next hypothesized that mutations in non-shared genes may also induce similar expression changes if they affect the same cellular processes or the same resistance mechanisms. To test this hypothesis, we classified the mutated genes into nine major resistance categories as previously (fig. 4*B*, supplementary data S3, Supplementary Material online; Lázár et al. 2014). Based on this categorization, we calculated the overlap in the mutated resistance categories across all pairs of antibiotic-adapted lines (fig. 4*B* and *C*). There was no significant correlation between transcriptome similarity and the extent of overlap in the mutated resistance categories (Spearman's rho = 0.13, $P = 0.07$, fig. 4*C*). A similar result was obtained when genetic similarity between antibiotic-adapted lines was calculated by classifying mutated genes into Gene Ontology (GO) categories instead of major resistance mechanisms (Spearman's rho = 0.09, $P = 0.24$, supplementary fig. S3, Supplementary Material online).

How to explain the broad transcriptome similarity of adapted lines mutated in functionally distinct genes? Inspection of the list of mutated genes revealed that they are frequently parts of the same regulatory unit involved in multidrug transport regulation (supplementary text S1, Supplementary Material online). For example, a line adapted to chloramphenicol (CHL9) carries mutations in genes affecting efflux pump activities (*marR*, *acrR*, and *acrB*), while another line adapted to ampicillin (AMP7) is mutated in *ompF*, which encodes an outer membrane porin. Intriguingly, the two lines show similar transcriptional changes (Pearson's $r = 0.63$), possibly due to *ompF* being a regulatory target of the MarAR system (Prajapat et al. 2015). More generally, we found that mutations either affected regulators, such as AcrR, EnvZ, MarR, OmpR, PhoQ, and SoxR, or their downstream-regulated genes that encode porins (OmpC, OmpF) and multidrug efflux pumps (AcrAB). Consequently, all of these mutations likely confer resistance by altering the uptake or efflux of antibiotics and thereby induce similar transcriptional changes.

Parallel Evolution of Extensive Transcriptome Rewiring

The results above show that adaptation to various unrelated antibiotics often yields similar gene expression

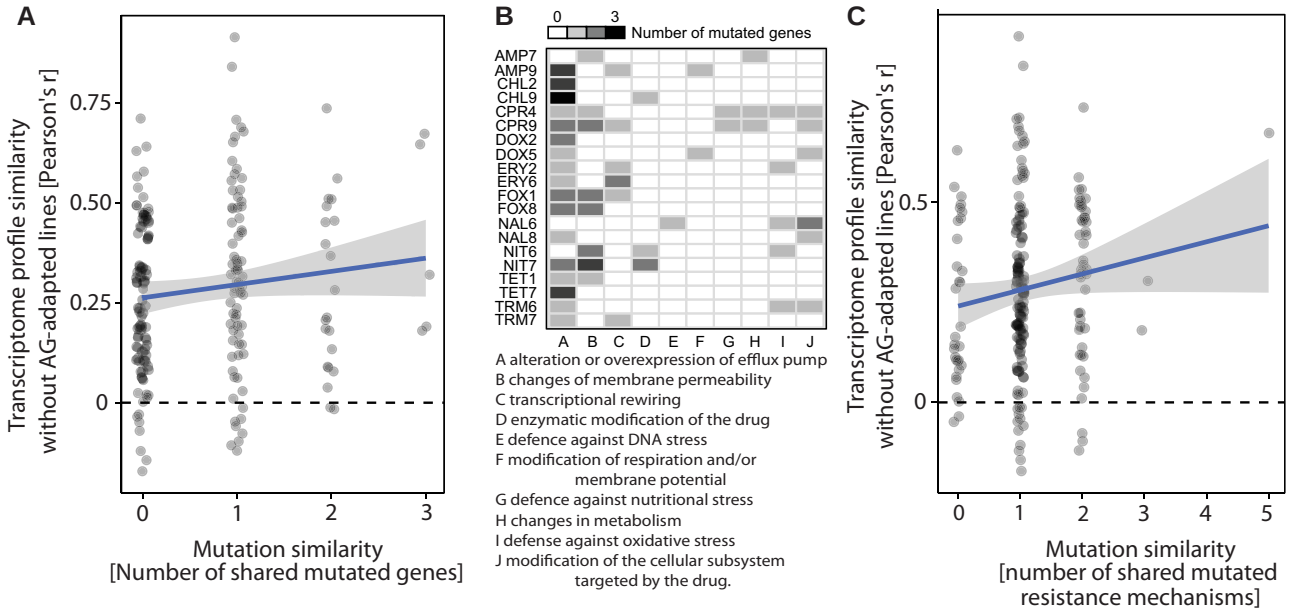

Fig. 4. Transcriptomic and genomic evolution are decoupled. (*A*) Mutation profile similarity at the level of genes (i.e., number of overlapping mutated genes) does not correlate with transcriptome profile similarity (without aminoglycoside-adapted lines, Spearman's rho = 0.11, $P = 0.14$). (*B*) Number of mutated genes in each resistance mechanism category across antibiotic-adapted lines (without aminoglycoside-adapted lines). (*C*) Mutation profile similarity at the level of resistance mechanism categories (i.e., number of shared mutated resistance mechanisms) shows no correlation with transcriptome profile similarity (without aminoglycoside-adapted lines, Spearman's rho = 0.13, $P = 0.07$).

changes. We hypothesize that evolutionary adaptation to antibiotic stresses elicits a limited repertoire of stereotypic global gene expression programs rather than unique, antibiotic-specific responses. Consistent with this hypothesis, the extent of transcriptional similarity between pairs of antibiotic-adapted lines show a marked positive correlation with the average number of differentially expressed genes in the two lines (without aminoglycoside-adapted lines, Spearman's rho = 0.46, $P < 0.0001$, supplementary fig. S4, Supplementary Material online). This suggests that the transcriptomic profiles of genotypes that show extensive gene expression rewiring are not unique but rather show strong parallelism between antibiotic-adapted lines. For example, lines adapted to tetracycline (TET1 and TET7) show massive gene expression rewiring, affecting >1,200 transcripts. Remarkably, the resulting transcriptomic profiles are similar not only to those of other 30S ribosome inhibitor adapted lines, but also to those adapted to cell wall and gyrase inhibitors (table 1, fig. 1*B*).

We next sought to understand the common properties of antibiotic-adapted lines showing extensive genomic expression changes. First, we asked whether such lines share mutations in specific genes. We found that lines with both high and low numbers of differentially expressed genes show similar sets of shared mutations (fig. 5*A* and *B*), hence recurrently mutated genes are unlikely to explain this difference. For example, mutations in the *acrAB* multidrug efflux pump genes occur frequently in lines with low and high numbers of differentially expressed genes alike. On the other hand, many genes were mutated in a single antibiotic-adapted line only (fig. 5*B*). Overall, these findings indicate that parallel evolution at the level of mutated genes is decoupled from parallelism at the transcriptomic level, potentially due to the existence of multiple alternative ways to induce similar gene expression changes.

Next, we systematically identified recurrent changes in the activity of transcriptional regulators across antibiotic-adapted lines. To this end, we made use of a set of 92 statistically independent transcriptomic modules that shape the expression of specific genes sets (Sastry et al. 2019). These transcriptomic modules were previously inferred, in an unbiased manner, from a diverse compendium of RNA-Seq data sets covering regulatory responses to various environmental and genetic perturbations (supplementary data S4, Supplementary Material online). Importantly, the majority of these modules correspond to known regulons and therefore represent the activity states of transcriptional regulators (Sastry et al. 2019). For each antibiotic-adapted line, we identified transcriptomic modules that show significantly altered activities compared with wild type based on its gene expression profile (fig. 5*C*, see Materials and Methods). We found several regulatory responses that are shared across antibiotic-adapted lines with large numbers of differentially expressed genes. These include, among others, enhanced activity of modules Fur-1, Fur-2, SoxS, and ArcA, which are involved in iron homeostasis, oxidative stress response, and respiration, respectively (Sastry et al. 2019). Indeed, the inferred activity of the SoxS module correlates well with the total number of significant gene expression changes across antibiotic-adapted lines (Pearson's $r = 0.58$, $P < 0.01$). These changes in module activities indicate

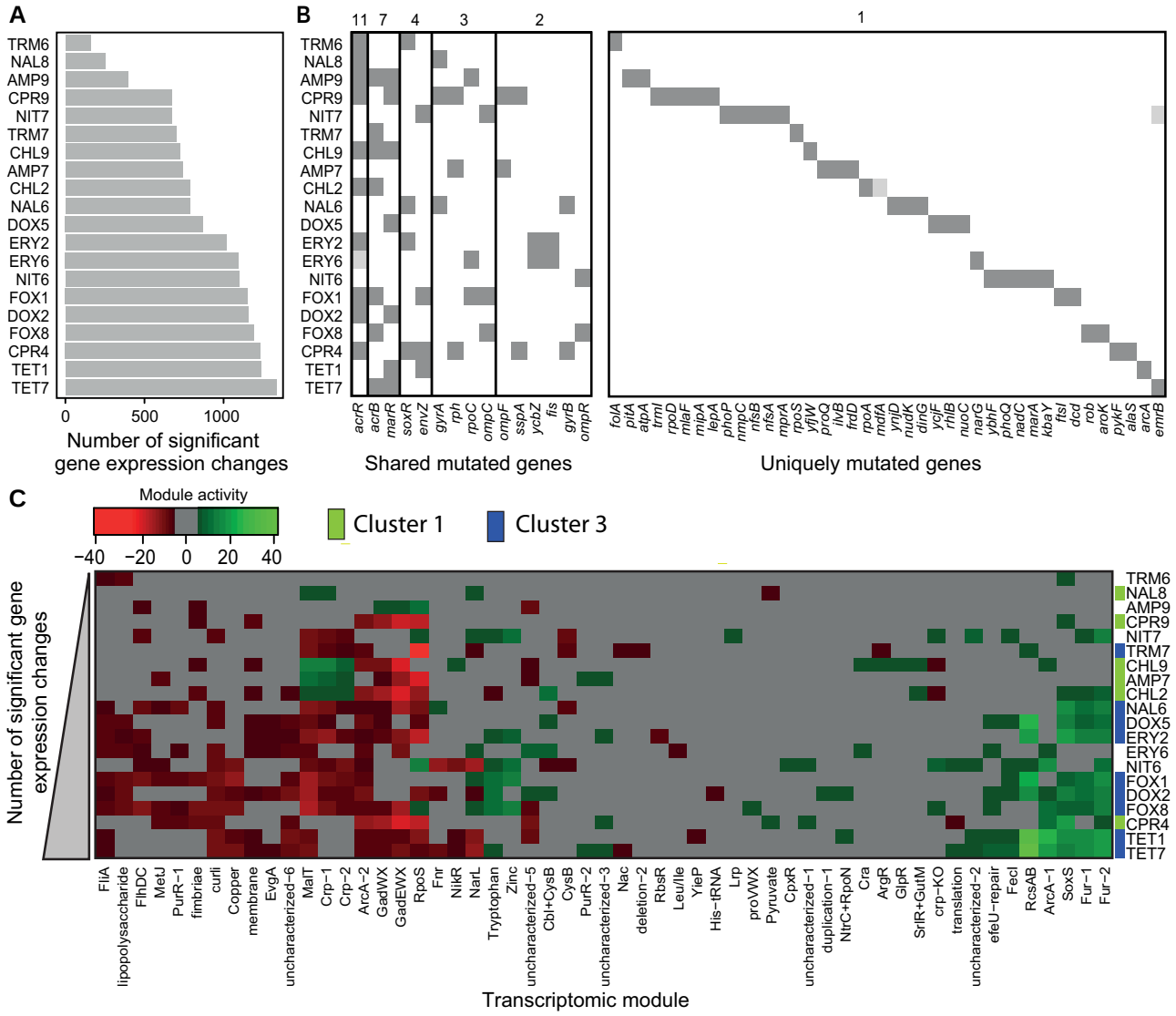

FIG. 5. Mutational profiles and regulatory activities of antibiotic-adapted lines. Antibiotic-adapted lines are ordered according to the total number of significant gene expression changes. Note that aminoglycoside-adapted lines were removed from this analysis as they show distinct mutational and transcriptional profiles from the rest of the genotypes. (*A*) Number of significant gene expression changes and (*B*) mutated genes across adapted lines. Numbers on the top represent the number of adapted lines in which a given gene is mutated. Overlapping mutations are present in lines with both high and low numbers of gene expression changes. Most lines contain one or more unique mutations as well. Note that NIT6* line also contains a large deletion spanning 41 genes (supplementary data S1, Supplementary Material online). Light gray indicates mutation in the promoter region of the corresponding gene. (*C*) Heatmap of altered transcriptomic module activities across antibiotic-adapted lines. Intensity values were calculated as previously described (Sastry et al. 2019; see Materials and Methods). Green color indicates increased, while red color indicates decreased activation of a transcriptomic module in a given genotype. For better visualization, modules showing no or mild changes are in gray color (i.e., values between −5 and 5). Colored stripes along the *y*-axis of the heatmap correspond to clusters identified in figure 1. Note that aminoglycoside-adapted lines (found in Cluster 2) were removed from the analysis.

alterations in metabolism linked to oxidative stress, as suggested before (Kohanski et al. 2010; Dwyer et al. 2014; Händel et al. 2016; Courtney et al. 2017). In addition, we report altered activity of a key transcriptional module (RcsAB) involved in colanic acid exopolysaccharide biosynthesis. Exopolysaccharides protect against osmotic and oxidative stress (Chen et al. 2004) and influence survival in the gastrointestinal environment (Mao et al. 2006). Finally, antibiotic-adapted lines with extensive gene expression changes share a common response that affects lipopolysaccharide (LPS) synthesis. This finding is consistent with a previous report that several of these antibiotic-adapted lines show enhanced susceptibility to the membrane-damaging agent bile acid and display altered expression in LPS-related genes (Lázár et al. 2018). Notably, while the above-listed regulatory changes are most prominent among antibiotic-adapted lines belonging to one particular transcriptomic cluster (Cluster 3, see fig. 1*B*), they also occur in various other lines with extensive expression changes (fig. 5*C*), suggesting that they represent recurrent regulatory alterations associated with global transcriptomic rewiring.

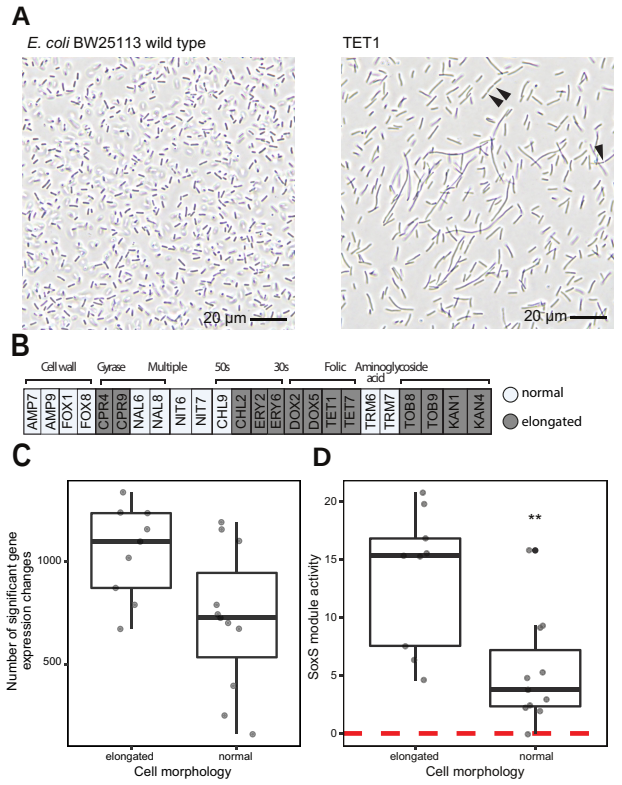

Fig. 6. Altered cell morphology in antibiotic-adapted lines. (*A*) The *Escherichia coli* K-12 BW25113 wild-type ancestor has normal cell shape, whereas several antibiotic-adapted lines, such as TET1, show highly elongated cell shapes. Arrowheads indicate divisome formation. (*B*) Lines adapted to the same antibiotic generally display similar cell morphology (i.e., either normal, like the wild-type ancestor; or elongated, like TET1). Most lines with elongated cell shape were adapted to ribosome inhibitors (aminoglycosides, 50*S* and 30*S* ribosome inhibitors). (*C*) Antibiotic-adapted lines with elongated cells show larger numbers of significant gene expression changes than those retaining a normal cell shape (Welch's test, $P < 0.05$, two-sided, without aminoglycoside-adapted lines). (*D*) Lines with elongated cells show an increased SoxS module activation compared with those with normal, wild type like morphology (Welch's test, $P < 0.01$, two sided, without aminoglycoside-adapted lines).

Taken together, these results suggest that resistance evolution in the laboratory often converges on a regulatory state with elevated oxidative stress response and altered cell surface composition. Conceivably, the antibiotic-adapted lines display extensive genome-wide transcriptional changes (fig. 1) because the altered regulatory modules influence the expression of numerous genes (Sastry et al. 2019).

Transcriptome Rewiring is Associated With Altered Cell Shape

Escherichia coli adopts an elongated cell shape in stressful environments where cells can grow but are unable to divide (Murashko and Lin-Chao 2017). Because our results above indicate that antibiotic-adapted lines frequently display a constitutively activated stress response (i.e., in the absence of antibiotics), we hypothesize that these lines may also show altered cell shapes. To test this, we analyzed cell shape under a non-stressed condition using light microscopy (see Materials and Methods). Remarkably, we found that over half of the antibiotic-adapted lines (14 out of 24) show abnormally long cells (supplementary data S3, Supplementary Material online). For example, cells of the TET1 line are markedly longer than wild type and form long filaments of incompletely separated cells (fig. 6*A*). Changes in cell shape are highly reproducible among parallel lines adapted toward the same antibiotic stress: in 11 out of 12 antibiotics, parallel lines show similar morphology (fig. 6*B*, supplementary data S3, Supplementary Material online).

In agreement with the hypothesis, we find that lines with elongated cells contain particularly high numbers of differentially expressed genes (fig. 6*C*, Welch's *t*-test, $P < 0.01$; without aminoglycoside-adapted lines $P < 0.05$), that include both up- and downregulations (Welch's *t*-test, $P = 0.044$ and $P = 0.013$ for up- and downregulated genes, respectively). We further hypothesize that this extensive regulatory rewiring may lead to activated stress response similar to that caused by exposure to hostile environment and thus results in elongated cells. Therefore, we systematically identified stress response modules that are specifically activated in antibiotic-adapted lines with elongated cells. We found that the SoxS stress module, which is related to oxidative stress is specifically activated in the elongated adapted lines (fig. 6*D*, supplementary data S4, Supplementary Material online). This finding is broadly consistent with previous studies indicating that activation of stress response could lead to stalled cell division and hence increased survival in various stressful environments (Miller 2004; Justice et al. 2008; Jones et al. 2013). Because antibiotic-adapted lines show an elongated morphology in the absence of antibiotics, these findings indicate that constitutive activation of stress response pathways leads to a permanent and inadequate perception of stresses and consequent alteration in cell shape. Notably, antibiotic-adapted lines with an elongated shape do not share any particular mutations, further supporting the role of common transcriptomic alterations underlying filamentous morphology (figs. 5*B* and 6*B*). Finally, we note that elongated cell morphology has likely been reached through multiple distinct mechanisms in our antibiotic-adapted lines. For example, the elongated shape of aminoglycoside-adapted lines (supplementary data S4, Supplementary Material online, fig. 6*B*) is unlikely to be driven by the above stereotypic expression changes, but could potentially be linked to the large fitness cost associated with aminoglycoside resistance.

Extensive Transcriptome Rewiring is Associated With Collateral Sensitivity to Antimicrobial Peptides

Finally, we asked whether the widespread gene expression changes induced by antibiotic resistance are associated with altered susceptibility to other antimicrobial compounds. Our results so far indicate that antibiotic-adapted lines with extensive gene expression changes have altered metabolism, outer membrane, and cell surface composition

and cell shape. These physiological alterations in turn may modulate the uptake and cellular toxicity of various drugs (Martínez and Rojo 2011; Ferreira and Kasson 2019; Nelson et al. 2020). For example, expression changes in LPS biosynthesis–related genes are associated with enhanced susceptibility to certain antimicrobial peptides (Lázár et al. 2018). Therefore, we hypothesize that such antibiotic-adapted lines might show altered susceptibility to an especially large number of antimicrobials.

To test the hypothesis, we focused on two distinct sets of antimicrobial agents: conventional antibiotics and antimicrobial peptides, which are promising alternative antimicrobials (Wang et al. 2019; Lazzaro et al. 2020). In our previous studies, we measured the susceptibility profiles of the antibiotic-adapted lines against 12 antibiotics (Lázár et al. 2014) and 24 antimicrobial peptides (Lázár et al. 2018) using high-throughput assays (supplementary data S4, Supplementary Material online). Both sets of compounds were selected to cover a broad range of mechanisms of action. The resulting data set provides qualitative information on the presence and absence of cross-resistance and collateral sensitivity interactions across antimicrobials (supplementary data S4, Supplementary Material online). Based on our previously published antibiotic susceptibility measurement (Lázár et al. 2014, 2018), we estimated the degrees of cross-resistance and collateral sensitivity for each antibiotic-adapted line by counting the number of antibiotics and antimicrobial peptides that show decreased and increased susceptibility to it, respectively. Remarkably, the extent of transcriptional changes shows a positive correlation with the number of collateral sensitivity interactions toward antimicrobial peptides (fig. 7*A*). We have previously shown that upregulation of LPS-related genes in antibiotic-adapted lines contributes to increased sensitivity toward certain antimicrobial peptides (Lázár et al. 2018, supplementary fig. S5, Supplementary Material online). Importantly, the correlation between the extent of transcriptional changes and the degree of collateral sensitivity toward antimicrobial peptides remains when removing LPS-related genes from the analysis (Spearman's rho = 0.55, $P < 0.05$). Indeed, genes belonging to several other functional categories show a similar association between the extent of transcriptional changes and degree of collateral sensitivity to antimicrobial peptides (supplementary data S5, Supplementary Material online). Among the functional classes, phosphotransferase activity, cellular iron ion homeostasis, sulfuric ester hydrolase, lipid A biosynthetic process, transmembrane transport activity, and membrane-related genes show the strongest correlations. Furthermore, antibiotic-adapted lines with extensive gene expression changes tend to show enhanced sensitivity to various pore forming and intracellular targeting peptides alike (supplementary data S4, Supplementary Material online). At the same time, these lines show few, if any, cross-resistances to antimicrobial peptides (fig. 7*B*). In contrast to these findings on antimicrobial peptides, the extent of transcriptional changes does not correlate with either the cross-resistance or collateral sensitivity degree against antibiotics (fig. 7*C* and *D*).

Collectively, these results suggest that antibiotic-adapted lines with numerous differentially expressed genes show a common physiological change that is associated with enhanced susceptibility to various antimicrobial peptides.

Discussion

In this work, we tested the hypothesis that antibiotic-resistance mutations cause widespread gene expression changes that in turn alter cellular phenotypes, including altered susceptibilities to other antimicrobial agents. We studied transcriptomic changes in laboratory-evolved antibiotic-resistant bacteria due to their tractability. We found that antibiotic-resistance mutations, including clinically relevant ones, frequently induce genome-wide gene expression changes in the absence of antibiotic stress. Notably, the extent of such constitutive transcriptomic changes is comparable with those induced by environmental stresses (Jozefczuk et al. 2010; Rau et al. 2016). Gene expression changes were repeatable even among lines adapted to functionally distinct antibiotics and those that have no mutated resistance genes in common, possibly due to convergent regulatory rewiring of the multidrug transport system. The resulting stereotypic expression changes include upregulation of regulatory modules involved in oxidative stress response, ferric ion homeostasis, and membrane-associated functions. Finally, we found that these gene expression alterations are associated with elongated cell shape and increased sensitivity to various antimicrobial peptides, suggesting that transcriptomic rewiring may mediate trade-offs between resistance phenotypes.

Constitutive activation of specific stress response regulons in antibiotic-adapted bacteria might be adaptive rather than simply a pleiotropic side effect of resistance mutations. Several links have been described between stress protection and antimicrobial-resistant determinants, including stress-dependent recruitments of efflux systems and LPS modification (Poole 2012). It is thus conceivable that at least some of the mutations that upregulate stress regulons had a selective advantage during laboratory evolution. Finally, while the observed gene expression alterations may incur some fitness cost, this is unlikely to be substantial because adapted lines with extensive transcriptomic alterations did not display particularly low fitness in the absence of antibiotic stress (supplementary fig. S1*B* and data S3, Supplementary Material online).

Prior works indicate that evolution of antibiotic resistance often induces collateral sensitivity toward antimicrobial peptides (Lee et al. 2009; Andersson et al. 2016; Lázár et al. 2018). It has been shown that specific collateral sensitivity interactions partly arise through regulatory changes affecting the LPS composition of the bacterial outer membrane (Lázár et al., 2018). Our results go beyond prior findings in two aspects. First, our data suggest that gene regulatory changes influence not only the sensitivity to specific antimicrobial peptides, but also the broader capacity

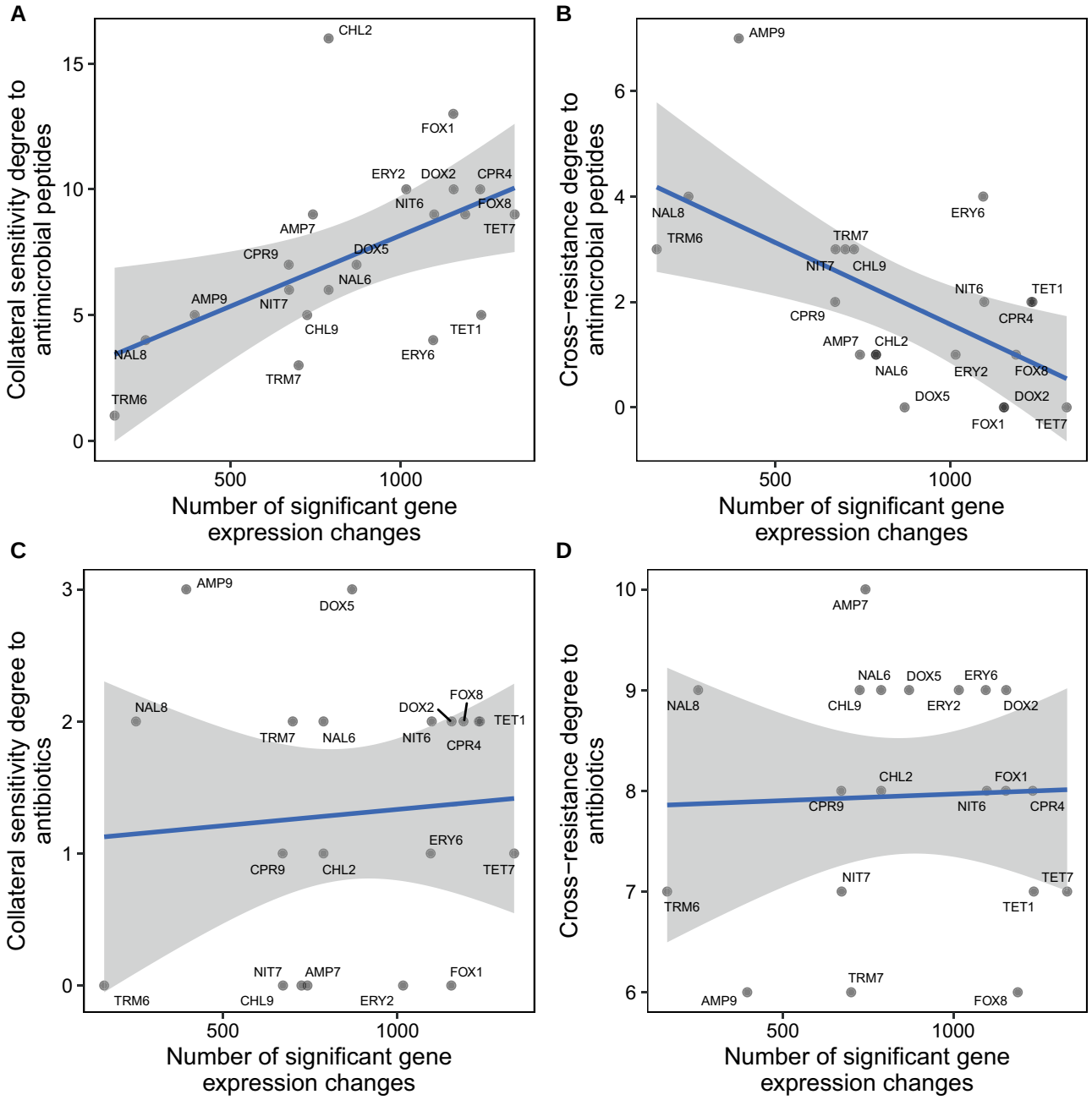

Fig. 7. Correlation between the extent of gene expression changes and degree of altered susceptibility to antimicrobial compounds. Plots show the numbers of cross-resistance and collateral sensitivity interactions (i.e., cross-resistance and collateral sensitivity degrees, respectively) as a function of the total number of significant gene expression changes across antibiotic-adapted lines ($N = 20$ adapted lines, without aminoglycoside-adapted ones). For antimicrobial peptides, (*A*) the degree of collateral sensitivity interactions positively correlates (Spearman's rho: 0.56, $P = 0.0103$), while (*B*) the degree of cross-resistance interactions negatively correlates (Spearman's rho: −0.60, $P = 0.005$). In the case of antibiotics, neither (*C*) the degree of collateral sensitivity (Spearman's rho = 0.16, $P = 0.49$) nor (*D*) the degree of cross-resistance interactions correlates (Spearman's rho = −0.02, $P = 0.94$) with the number of significant gene expression changes.

to tolerate various classes of antimicrobial peptides. In particular, antibiotic-adapted bacteria with widespread gene expression alterations tend to show enhanced sensitivity to multiple antimicrobial peptides, including both pore forming and intracellular targeting peptides (supplementary data S4, Supplementary Material online). Second, increased sensitivity toward antimicrobial peptides is associated with regulatory changes in various cellular subsystems beyond LPS-related gene functions. For example, gene expression changes in ferric ion binding proteins and transmembrane transporters are predictive of the breadth of collateral sensitivity to antimicrobial peptides. Clearly, further studies are needed to test the causal involvement of these gene expression changes in antimicrobial peptide susceptibilities and to decipher their molecular mechanisms. Finally, we note that while the ancestral strain background (BW25113) used in the present study is widely employed to study the mechanistic aspects

of AMP susceptibility (Ebbensgaard et al. 2015, 2018; Krizsan et al. 2015; Lázár et al. 2018), it is unable to synthesize the O-antigen (Browning et al. 2013) and therefore the relevance of our findings to clinical isolates remains to be tested.

Our work has implications to our understanding of the links between bacterial cellular morphology and antibiotic treatments. Bacterial cells often adopt an elongated shape upon exposure to various stresses, including antimicrobial agents (Justice et al. 2008). Such morphological changes are thought to enhance survival under stressful conditions and play a crucial role in subverting the host immune response in pathogenic *E. coli* (Justice et al. 2006). Our results indicate that evolutionary adaptation to antibiotic stresses frequently leads to an elongated cell shape in non-stressed conditions. Elongated morphology showed a close association with induction of oxidative and heat stress responses, suggesting that a constitutively active stress response may underlie this phenotype. This hypothesis is broadly consistent with previous examples showing a link between the induction of DNA damage response and elongated bacterial forms (Justice et al. 2008). It has also been proposed that elongation might be the first step in the evolution of resistance to mutagenic antibiotic exposure (Bos et al. 2015). A key open issue is whether the accumulation of resistance mutations also alters cell shape in clinical isolates. If so, it might offer a strategy to rapidly detect resistant bacteria by monitoring cell morphology (Otero et al. 2017).

Finally, our results have implications for the interplay between phenotypic plasticity and adaptive evolution of genomic expression. It has been debated whether plastic gene expression changes act as stepping stones to genetic adaptation when the organism encounters a new environment (Ho and Zhang 2018) and whether selection acts to render the plastic response constitutive (i.e., genetic assimilation; Schlichting and Wund 2014; Horinouchi et al. 2017). We found that the initial plastic transcriptomic response upon antibiotic stress is markedly different from the constitutive transcriptomic changes evolved as a result of accumulating resistance mutations. This finding indicates that the constitutive gene expression states reached by antibiotic adaptation are unlikely be the result of genetic assimilation of the initial plastic response, at least on the evolutionary time scale of our laboratory study. Furthermore, this result is broadly consistent with recent observations that plastic gene expression changes do not typically act as stepping stones for genetic adaptations in experimental evolutionary studies (Ho and Zhang 2018). Nevertheless, we wish to emphasize that further studies involving transcriptome profiling of antibiotic-adapted lines in the presence of antibiotic stresses would be needed to more directly test the stepping stone hypothesis.

In sum, our work establishes that adaptation to various classes of antibiotics often leads to global regulatory rewiring that converges on similar gene expression profiles. We propose that these regulatory changes in turn influence the cellular morphology and antimicrobial susceptibility of resistant bacteria.

Materials and Methods

Genotypes

Antibiotic-adapted and single-mutant lines were obtained from our previous laboratory adaptation experiment (Lázár et al. 2013). Briefly, lines were parallel evolved under the same physical conditions and the same chemically defined medium supplemented with one of the 12 antibiotics, similar to other studies (Oz et al. 2014; Tenaillon et al. 2016; Horinouchi et al. 2017). *Escherichia coli* K-12 BW25113 was used as the wild-type ancestor during the laboratory adaptation as well as in the transcriptomic analysis. Altogether 24 antibiotic-adapted lines (2 adapted lines per antibiotic) and 7 single mutants (lines carrying a single antibiotic-resistance mutation identified in one of the antibiotic-adapted lines) were chosen for transcriptomic analysis. Antibiotic-adapted lines exhibit MICs up to 328-fold above that of the wild-type ancestor, well above the current clinical breakpoints according to EUCAST or the European Reference Laboratory for Antimicrobial Resistance. Whole-genome sequencing results are available from our previous studies for all 24 adapted lines (Lázár et al. 2013, 2014) The seven *E. coli* single-mutant lines carrying one of the following resistance mutations: envZ[Ala396Thr], marR[Val84Glu], trkH[Thr350Lys], gyrA[Asp87Gly], phoQ[Gly384Cys], rpoC[Ala784Val], and soxR[Leu139*] were established using a highly precise allele replacement protocol (Toprak et al. 2012; Lázár et al. 2013; Nyerges et al. 2016). All antibiotic-adapted and single-mutant lines as well as the wild-type ancestor were preserved at 80 °C in 20% (v/v) glycerol solution.

Medium and Total RNA Isolation

For obtaining the RNA samples, the antibiotic-adapted and single-mutant lines, as well as the wild type, were grown in the same medium as during the evolutionary experiments, but without adding any antibiotics (i.e., autoclaved MS-minimal medium supplemented with 0.2% glucose and 0.1% casamino acids). To ensure that transcriptomic measurements are comparable across different genotypes, total RNA were collected in log-phase ($A_{600\ nm} \approx 1$) from samples grown in minimal medium devoid of any antibiotic. Total RNA was isolated as described previously (Méhi et al. 2014). In short, isolation was performed using NucleoSpin RNA extraction kit (Macherey-Nagel), then the purity was determined as 260 nm/280 nm absorbance ratio (expected ≈ 2) using NanoDrop 1000 spectrophotometer (Thermo Scientific). RNA integrity measurement was done by using 1% agarose gel electrophoresis with GelRed staining. Then, the remaining genomic DNA were eliminated using Ambion DNase I (Ambion).

Whole Transcriptome Sequencing and Data Analysis

Whole transcriptome sequencing was performed on 24 antibiotic-adapted lines (2 lines per antibiotic), 7 single mutation carrying lines and the ciprofloxacin-treated wild-type ancestor. The transcriptomes of the 24

antibiotic-adapted lines were analyzed and published in our previous work (Lázár et al. 2018). Here we used the same RNA extraction, sequencing and data analysis method for the analysis of the additional set of seven single-mutant lines and the ciprofloxacin-treated wild-type ancestor strain as described previously (Lázár et al. 2018). In the case of ciprofloxacin treatment, before RNA isolation, log-phase cells of the ancestor were treated with a lethal concentration of ciprofloxacin (50 ng/ml) for 120 min. These samples were then compared with those obtained immediately before ciprofloxacin treatment. Three biological replicates were used for both the adapted, the single-mutant lines, as well as for ciprofloxacin treatment, while the untreated wild-type control was represented by 15 biological replicates. Raw sequence has been quality filtered and the mapped read counts for each annotated gene has been calculated using U00096.3 reference genome sequence and *E. coli* strain K-12 MG1655 annotation (Zhou and Rudd 2013; Lázár et al. 2018). All of the programs and parameters used to estimate gene expression can be found in our previous study (Lázár et al. 2018). In the next steps, genes with low expression level (keeping only those genes that were detected by at least five mapped reads in at least 25% of the samples included in the study) along with ribosomal genes were removed from the analysis. R version 3.0.2 (2013) is used for data normalization (Robinson et al. 2010), Log transformation, and quantile normalization (Ritchie et al. 2015; using "trimmed mean of M-values" method—Robinson and Oshlack 2010) and "ComBat" tool from the "sva" package version 3.8.053 for the correction of the systematic batch effect as described previously (Lázár et al. 2018). Subsequently, empirical Bayes moderation and calculation of differentially expressed genes were carried out using "limma" (Ritchie et al. 2015).

Differentially expressed genes were identified based on the comparison of the normalized counts per read of the control and the other lines. Genes considered as differentially expressed when the false-discovery rate corrected *P*-values were below threshold (corrected *P*-values <0.05) and also had greater FC than a chosen threshold ($|\log_2(FC)|>1$). The $\log_2$ FC values of the normalized expression data and the false-discovery rate corrected *P* values are provided in supplementary data S2, Supplementary Material online.

Log_2 FC values of the genes were used for clustering the 7 single mutant and the 24 antibiotic-adapted lines. Ensemble method with Euclidean distance measure was adapted for gene-wise clustering, while clustering of genotypes was performed using the Ward method with 1 - Pearson's r as a distance measure (Murtagh and Legendre 2014).

To analyze the transcriptomic response of the wild-type BW25113 strain background to sublethal dose of antibiotic stress, we collected processed transcriptomic data for 5 antibiotic treatments from a previous transcriptome sequencing study (Zoffmann et al. 2019) (supplementary data S2, Supplementary Material online).

The transcriptome data can be accessed from the Gene Expression Omnibus repository (https://www.ncbi.nlm.nih.gov/geo/) with accession number GSE96706 and GSE223493.

Measurement of Regulatory Module Activity

As most of the gene expression changes are likely caused by alterations in the underlying regulatory network, we estimated changes in the activity of independent regulatory modules based on a previous study (Sastry et al. 2019). In that study, a diverse compendium of high-quality *E. coli* RNA-Seq data sets were subjected to signal decomposition to identify gene sets that are independently modulated at constant ratios across all conditions, referred to as modules here and mathematically represented as a matrix of independent components (Sastry et al. 2019). Importantly, most of these modules correspond to specific regulons associated with the activities of specific transcription factors. Using our gene expression data and the independent components matrix, we inferred the relative activity of these 92 statistically independent modules in our genotypes. First, we filtered out the non-overlapping genes between the independent components matrix (*S*-matrix) and the matrix (X) containing our 31 expression profiles and we kept 3,923 genes. We used the following formula to estimate modulon activity:

$$A = pinv(S)^{*}X$$

where A represents the activities of the modules for the 31 genotypes and *pinv* is the pseudo-inverse function (Ben-Israel and Greville 2003). Matrix A is provided in supplementary data S4, Supplementary Material online.

Microscopic Analysis

The 24 antibiotic-adapted, the 7 single-mutant lines, as well as the wild-type ancestor were grown in autoclaved MS-minimal medium supplemented with 0.2% glucose and 0.1% casamino acids and incubated at 30 °C in 96-well plate with shaking at 300 rpm. After mounting the cells, images were captured using Nikon Eclipse 80i microscope with a 100× oil immersion lens.

Supplementary material

Supplementary data are available at *Molecular Biology and Evolution* online.

Acknowledgments

This work was supported by the "Lendület" program of the Hungarian Academy of Sciences LP-2009-013/2012 (B.P.), LP-2012-32/2018 (C.P.), the ELKH Lendület program LP-2017-2010/2020 (C.P.), the Wellcome Trust WT 098016/Z/11/Z (B.P.), The European Research Council H2020-ERC-2014-CoG 648364-Resistance Evolution (C.P.), and H2020-ERC-2019-PoC 862077-Aware (C.P.), the

National Research, Development and Innovation Office and the Ministry for Innovation and Technology under the "Frontline" program KKP KH125616 and 126506 (B.P. and C.P.), RRF-2.3.1-21-2022-00006 (B.P.), GINOP-2.3.2 -15-2016-00026 (iChamber, B.P.), GINOP-2.3.2-15-2 016-00014 (EVOMER, C.P. and B.P.), GINOP-2.3.2-15-2 016-00020 (MolMedEx TUMORDNS, C.P.), National Laboratory of Biotechnology Grant 2022-2.1.1-NL-2022 -00008 (C.P. and B.P.), The European Union's Horizon 202 0 research and innovation program under grant agreement No 739593 (B.P.). NKFIH grant FK124254 (O.M.), the Janos Bolyai Research Fellowship from the Hungarian Academy of Sciences BO/608/21 (R.S.).

Author ContributionsNational Research, Development and Innovation Office

B.P. and C.P. conceived and supervised the project. R.S. and O.M. purified RNA for transcriptomic analysis. B.B. and I.N. performed RNA-Seq experiments. G.G. and B.P. analyzed the data. B.P., C.P., G.G., and R.S. wrote the paper. V.L., R.S., and A.D. contributed to all other experiments. G.G., R.S., A.D., V.L., B.P., and C.P. interpreted the data.

Data Availability

The raw genome sequences of the 24 antibiotic-adapted lines have been deposited in NCBI Bioproject database under the accession code PRJNA248327 (accession SRP042209) as published in our previous work (Lázár et al. 2014).

Conflict of interest statement

Authors declare that they have no competing interests. B.B. and I.N. had consulting positions at SeqOmics Biotechnology Ltd. at the time the study was conceived. SeqOmics Biotechnology Ltd. was not directly involved in the design and execution of the experiments or in the writing of the manuscript.

References

Adler M, Anjum M, Andersson DI, Sandegren L. 2016. Combinations of mutations in envZ, ftsI, mrdA, acrB and acrR can cause high-level carbapenem resistance in *Escherichia coli*. *J Antimicrob Chemother*. **71**:1188–1198.

Andersson DI, Hughes D. 2010. Antibiotic resistance and its cost: is it possible to reverse resistance? *Nat Rev Microbiol*. **8**:260–271.

Andersson DI, Hughes D, Kubicek-Sutherland JZ. 2016. Mechanisms and consequences of bacterial resistance to antimicrobial peptides. *Drug Resist Updat*. **26**:43–57.

Andersson DI, Levin BR. 1999. The biological cost of antibiotic resistance. *Curr Opin Microbiol*. **2**:489–493.

Baym M, Lieberman TD, Kelsic ED, Chait R, Gross R, Yelin I, Kishony R. 2016. Spatiotemporal microbial evolution on antibiotic landscapes. *Science* **353**:1147–1151.

Ben-Israel A, Greville TNE. 2003. *Generalized inverses – theory and applications*. New York: Springer-Verlag.

Bos J, Zhang Q, Vyawahare S, Rogers E, Rosenberg SM, Austin RH. 2015. Emergence of antibiotic resistance from multinucleated bacterial filaments. *Proc Natl Acad Sci U S A*. **112**:178–183.

Browning DF, Wells TJ, França FLS, Morris FC, Sevastsyanovich YR, Bryant JA, Johnson MD, Lund PA, Cunningham AF, Hobman JL, *et al*. 2013. Laboratory adapted *Escherichia coli* K-12 becomes a pathogen of *Caenorhabditis elegans* upon restoration of O antigen biosynthesis. *Mol Microbiol*. **87**:939–950.

Chen J, Lee SM, Mao Y. 2004. Protective effect of exopolysaccharide colanic acid of *Escherichia coli* O157:H7 to osmotic and oxidative stress. *Int J Food Microbiol*. **93**:281–286.

Courtney CM, Goodman SM, Nagy TA, Levy M, Bhusal P, Madinger NE, Detweiler CS, Nagpal P, Chatterjee A. 2017. Potentiating antibiotics in drug-resistant clinical isolates via stimuli-activated superoxide generation. *Sci Adv*. **3**:e1701776.

Dunai A, Spohn R, Farkas Z, Lázár V, Györkei Á, Apjok G, Boross G, Szappanos B, Grézal G, Faragó A, *et al*. 2019. Rapid decline of bacterial drug-resistance in an antibiotic-free environment through phenotypic reversion. *eLife* **8**:e47088.

Dwyer DJ, Belenky PA, Yang JH, MacDonald IC, Martell JD, Takahashi N, Chan CTY, Lobritz MA, Braff D, Schwarz EG, *et al*. 2014. Antibiotics induce redox-related physiological alterations as part of their lethality. *Proc Natl Acad Sci U S A*. **111**:E2100–E2109.

Ebbensgaard A, Mordhorst H, Aarestrup FM, Hansen EB. 2018. The role of outer membrane proteins and lipopolysaccharides for the sensitivity of *Escherichia coli* to antimicrobial peptides. *Front Microbiol*. **9**:2153.

Ebbensgaard A, Mordhorst H, Overgaard MT, Nielsen CG, Aarestrup FM, Hansen EB. 2015. Comparative evaluation of the antimicrobial activity of different antimicrobial peptides against a range of pathogenic bacteria. *PLoS One*. **10**:e0144611.

Ehrenreich IM, Pfennig DW. 2016. Genetic assimilation: a review of its potential proximate causes and evolutionary consequences. *Ann Bot*. **117**:769–779.

Ferreira RJ, Kasson PM. 2019. Antibiotic uptake across gram-negative outer membranes: better predictions towards better antibiotics. *ACS Infect Dis*. **5**:2096–2104.

Händel N, Hoeksema M, Mata MF, Brul S, ter Kuile BH. 2016. Effects of stress, reactive oxygen species, and the SOS response on de novo acquisition of antibiotic resistance in *Escherichia coli*. *Antimicrob Agents Chemother*. **60**:1319–1327.

Ho W-C, Zhang J. 2018. Evolutionary adaptations to new environments generally reverse plastic phenotypic changes. *Nat Commun*. **9**:350–350.

Horinouchi T, Suzuki S, Kotani H, Tanabe K, Sakata N, Shimizu H, Furusawa C. 2017. Prediction of cross-resistance and collateral sensitivity by gene expression profiles and genomic mutations. *Sci Rep*. **7**:14009–14009.

Imamovic L, Ellabaan MMH, Dantas Machado AM, Citterio L, Wulff T, Molin S, Krogh Johansen H, Sommer MOA. 2018. Drug-driven phenotypic convergence supports rational treatment strategies of chronic infections. *Cell* **172**:121–134.e14.

Jones TH, Vail KM, McMullen LM. 2013. Filament formation by foodborne bacteria under sublethal stress. *Int J Food Microbiol*. **165**:97–110.

Jozefczuk S, Klie S, Catchpole G, Szymanski J, Cuadros-Inostroza A, Steinhauser D, Selbig J, Willmitzer L. 2010. Metabolomic and transcriptomic stress response of *Escherichia coli*. *Mol Syst Biol*. **6**:364.

Justice SS, Hunstad DA, Cegelski L, Hultgren SJ. 2008. Morphological plasticity as a bacterial survival strategy. *Nat Rev Microbiol*. **6**: 162–168.

Justice SS, Hunstad DA, Seed PC, Hultgren SJ. 2006. Filamentation by *Escherichia coli* subverts innate defenses during urinary tract infection. *Proc Natl Acad Sci U S A*. **103**:19884–19889.

Kohanski MA, Dwyer DJ, Collins JJ. 2010. How antibiotics kill bacteria: from targets to networks. *Nat Rev Microbiol*. **8**:423–435.

Kohanski MA, Dwyer DJ, Hayete B, Lawrence CA, Collins JJ. 2007. A common mechanism of cellular death induced by bactericidal antibiotics. *Cell* **130**:797–810.

Koutsolioutsou A, Peña-Llopis S, Demple B. 2005. Constitutive soxR mutations contribute to multiple-antibiotic resistance in clinical *Escherichia coli* isolates. *Antimicrob Agents Chemother*. **49**:2746–2752.

Krizsan A, Knappe D, Hoffmann R. 2015. Influence of the yjiL-mdtM gene cluster on the antibacterial activity of proline-rich antimicrobial peptides overcoming *Escherichia coli* resistance induced by the missing SbmA transporter system. *Antimicrob Agents Chemother*. **59**:5992–5998.

Lázár V, Martins A, Spohn R, Daruka L, Grézal G, Fekete G, Számel M, Jangir PK, Kintses B, Csörgő B, *et al.* 2018. Antibiotic-resistant bacteria show widespread collateral sensitivity to antimicrobial peptides. *Nat Microbiol*. **3**:718.

Lázár V, Nagy I, Spohn R, Csörgő B, Györkei Á, Nyerges Á, Horváth B, Vörös A, Busa-Fekete R, Hrtyan M, *et al.* 2014. Genome-wide analysis captures the determinants of the antibiotic cross-resistance interaction network. *Nat Commun*. **5**:4352.

Lázár V, Pal Singh G, Spohn R, Nagy I, Horváth B, Hrtyan M, Busa-Fekete R, Bogos B, Méhi O, Csörgő B, *et al.* 2013. Bacterial evolution of antibiotic hypersensitivity. *Mol Syst Biol*. **9**:700–700.

Lazzaro BP, Zasloff M, Rolff J. 2020. Antimicrobial peptides: application informed by evolution. *Science* **368**:eaau5480.

Lee J-H, Lee K-L, Yeo W-S, Park S-J, Roe J-H. 2009. SoxRS-mediated lipopolysaccharide modification enhances resistance against multiple drugs in *Escherichia coli*. *J Bacteriol*. **191**:4441–4450.

Mao Y, Doyle MP, Chen J. 2006. Role of colanic acid exopolysaccharide in the survival of enterohaemorrhagic *Escherichia coli* O157:H7 in simulated gastrointestinal fluids. *Lett Appl Microbiol*. **42**:642–647.

Martínez JL, Rojo F. 2011. Metabolic regulation of antibiotic resistance. *FEMS Microbiol Rev*. **35**:768–789.

Matsumoto Y, Murakami Y, Tsuru S, Ying B-W, Yomo T. 2013. Growth rate-coordinated transcriptome reorganization in bacteria. *BMC Genomics* **14**:808.

Méhi O, Bogos B, Csörgő B, Pál F, Nyerges A, Papp B, Pál C. 2014. Perturbation of iron homeostasis promotes the evolution of antibiotic resistance. *Mol Biol Evol*. **31**:2793–2804.

Miller C. 2004. SOS response induction by -lactams and bacterial defense against antibiotic lethality. *Science* **305**:1629–1631.

Mizuno T, Mizushima S. 1990. Signal transduction and gene regulation through the phosphorylation of two regulatory components: the molecular basis for the osmotic regulation of the porin genes. *Mol Microbiol*. **4**:1077–1082.

Murashko ON, Lin-Chao S. 2017. Escherichia coli responds to environmental changes using enolasic degradosomes and stabilized DicF sRNA to alter cellular morphology. *Proc Natl Acad Sci U S A*. **114**:E8025–E8034.

Murtagh F, Legendre P. 2014. Ward's hierarchical agglomerative clustering method: which algorithms implement Ward's criterion? *J Classif*. **31**:274–295.

Nelson N, Opene B, Ernst RK, Schwartz DK. 2020. Antimicrobial peptide activity is anticorrelated with lipid a leaflet affinity. *PLoS One*. **15**:e0242907.

Nyerges Á, Csörgő B, Nagy I, Bálint B, Bihari P, Lázár V, Apjok G, Umenhoffer K, Bogos B, Pósfai G, *et al.* 2016. A highly precise and portable genome engineering method allows comparison of mutational effects across bacterial species. *Proc Natl Acad Sci U S A*. **113**:2502–2507.

Otero F, Santiso R, Tamayo M, Fernández JL, Bou G, Lepe JA, McConnell MJ, Gosálvez J, Cisneros JM. 2017. Rapid detection of antibiotic resistance in gram-negative bacteria through assessment of changes in cellular morphology. *Microb Drug Resist Larchmt N*. **23**:157–162.

Oz T, Guvenek A, Yildiz S, Karaboga E, Tamer YT, Mumcuyan N, Ozan VB, Senturk GH, Cokol M, Yeh P, *et al.* 2014. Strength of selection pressure is an important parameter contributing to the complexity of antibiotic resistance evolution. *Mol Biol Evol*. **31**:2387–2401.

Pál C, Papp B, Lázár V. 2015. Collateral sensitivity of antibiotic-resistant microbes. *Trends Microbiol*. **23**:401–407.

Piddock LJV. 2006. Multidrug-resistance efflux pumps ? not just for resistance. *Nat Rev Microbiol*. **4**:629–636.

Poole K. 2012. Bacterial stress responses as determinants of antimicrobial resistance. *J Antimicrob Chemother*. **67**:2069–2089.

Prajapat MK, Jain K, Saini S. 2015. Control of MarRAB operon in *Escherichia coli* via autoactivation and autorepression. *Biophys J*. **109**:1497–1508.

Randall LP, Woodward MJ. 2002. The multiple antibiotic resistance (mar) locus and its significance. *Res Vet Sci*. **72**:87–93.

Rau MH, Calero P, Lennen RM, Long KS, Nielsen AT. 2016. Genome-wide *Escherichia coli* stress response and improved tolerance towards industrially relevant chemicals. *Microb Cell Factories*. **15**:176.

R Core Team. 2013. R: A language and environment for statistical computing. Available from: https://www.R-project.org/

Ritchie ME, Phipson B, Wu D, Hu Y, Law CW, Shi W, Smyth GK. 2015. Limma powers differential expression analyses for RNA-sequencing and microarray studies. *Nucleic Acids Res*. **43**:e47.

Robinson MD, McCarthy DJ, Smyth GK. 2010. Edger: a bioconductor package for differential expression analysis of digital gene expression data. *Bioinforma Oxf Engl*. **26**:139–140.

Robinson MD, Oshlack A. 2010. A scaling normalization method for differential expression analysis of RNA-seq data. *Genome Biol*. **11**:R25.

Sastry AV, Gao Y, Szubin R, Hefner Y, Xu S, Kim D, Choudhary KS, Yang L, King ZA, Palsson BO. 2019. The *Escherichia coli* transcriptome mostly consists of independently regulated modules. *Nat Commun*. **10**:5536.

Schlichting CD, Wund MA. 2014. Phenotypic plasticity and epigenetic marking: an assessment of evidence for genetic accommodation. *Evolution* **68**:656–672.

Schmidt A, Kochanowski K, Vedelaar S, Ahrné E, Volkmer B, Callipo L, Knoops K, Bauer M, Aebersold R, Heinemann M. 2016. The quantitative and condition-dependent *Escherichia coli* proteome. *Nat Biotechnol*. **34**:104–110.

Seo SW, Gao Y, Kim D, Szubin R, Yang J, Cho B-K, Palsson BO. 2017. Revealing genome-scale transcriptional regulatory landscape of OmpR highlights its expanded regulatory roles under osmotic stress in Escherichia coli K-12 MG1655. *Sci Rep*. **7**:2181.

Suzuki S, Horinouchi T, Furusawa C. 2014. Prediction of antibiotic resistance by gene expression profiles. *Nat Commun*. **5**:5792–5792.

Taber HW, Mueller JP, Miller PF, Arrow AS. 1987. Bacterial uptake of aminoglycoside antibiotics. *Microbiol Rev*. **51**:439–457.

Tenaillon O, Barrick JE, Ribeck N, Deatherage DE, Blanchard JL, Dasgupta A, Wu GC, Wielgoss S, Cruveiller S, Médigue C, *et al.* 2016. Tempo and mode of genome evolution in a 50,000-generation experiment. *Nature* **536**:165–170.

Toprak E, Veres A, Michel J-B, Chait R, Hartl DL, Kishony R. 2012. Evolutionary paths to antibiotic resistance under dynamically sustained drug selection. *Nat Genet*. **44**:101–105.

Vigne P, Gimond C, Ferrari C, Vielle A, Hallin J, Pino-Querido A, El Mouridi S, Mignerot L, Frøkjær-Jensen C, Boulin T, *et al.* 2021. A single-nucleotide change underlies the genetic assimilation of a plastic trait. *Sci Adv*. **7**:eabd9941.

Vila J, Ruiz J, Marco F, Barcelo A, Goñi P, Giralt E, Jimenez de Anta T 1994. Association between double mutation in gyrA gene of ciprofloxacin-resistant clinical isolates of *Escherichia coli* and MICs. *Antimicrob Agents Chemother*. **38**:2477–2479.

Vincent BM, Lancaster AK, Scherz-Shouval R, Whitesell L, Lindquist S. 2013. Fitness trade-offs restrict the evolution of resistance to amphotericin B. *PLoS Biol*. **11**:e1001692.

Waddington CH. 1953. Genetic assimilation of an acquired character. *Evolution* **7**:118–126.

Waddington CH. 1961. Genetic assimilation. *Adv Genet*. **10**:257–293.

Wang J, Dou X, Song J, Lyu Y, Zhu X, Xu L, Li W, Shan A. 2019. Antimicrobial peptides: promising alternatives in the post feeding antibiotic era. *Med Res Rev*. **39**:831–859.

Webber MA, Piddock LJ. 2001. Absence of mutations in marRAB or soxRS in acrB-overexpressing fluoroquinolone-resistant clinical and veterinary isolates of *Escherichia coli*. *Antimicrob Agents Chemother*. **45**:1550–1552.

Webber MA, Ricci V, Whitehead R, Patel M, Fookes M, Ivens A, Piddock JV. 2013. Clinically relevant mutant DNA gyrase alters

supercoiling, changes the transcriptome, and confers multidrug resistance. *mBio* **4**:e00273-13.
Wu J, Weiss B. 1991. Two divergently transcribed genes, soxR and soxS, control a superoxide response regulon of *Escherichia coli*. *J Bacteriol*. **173**:2864–2871.
Zhou J, Rudd KE. 2013. Ecogene 3.0. *Nucleic Acids Res*. **41**:D613–D624.
Zoffmann S, Vercruysse M, Benmansour F, Maunz A, Wolf L, Blum Marti R, Heckel T, Ding H, Truong HH, Prummer M, *et al*. 2019. Machine learning-powered antibiotics phenotypic drug discovery. *Sci Rep*. **9**:5013.